Eur. Phys. J. E **7**, 209–220 (2002)
DOI 10.1140/epje/i200101129

THE EUROPEAN PHYSICAL JOURNAL E
EDP Sciences

Dilution series approach for investigation of microstructural properties and particle interactions in high-quality magnetic fluids

M. Raşa[1,2,a], D. Bica[2,3], A. Philipse[1], and L. Vékás[2,3]

[1] Van 't Hoff Laboratory for Physical and Colloid Chemistry, Debye Institute, Utrecht University, Padualaan 8 3584 CH Utrecht, The Netherlands
[2] Institute for Complex Fluids, "Politehnica" University of Timişoara, Bd. Mihai Viteazul 1, Timişoara-1900, Romania
[3] Center for Fundamental and Advanced Technical Research, Romanian Academy of Science, Timişoara Branch Bd. Mihai Viteazul 24, Timişoara-1900, Romania

Received 27 August 2001

Abstract. The aim of the paper is to study the deviation of magnetic properties of the magnetic fluids prepared for this study, from ideal (Langevin) behaviour, *i.e.* to estimate particle interaction influence and dimensions and influence of particle aggregates, as well as to explain the related effects observed. We also determine the particle coupling parameter, the particle nonmagnetic layer thickness, and the particle distribution, which are fundamental for sample characterization. A comparison of the studied magnetic fluids with each other, with respect to microstructure formation and particle interaction strength is finally done. For these purposes, a concentration dependence study, following the proposed "dilution series approach", is performed. Three series of dilutions of three types of magnetic fluids were prepared and analyzed.

PACS. 75.50.Mm Magnetic liquids – 75.60.Ej Magnetization curves, hysteresis, Barkhausen and related effects – 82.70.Dd Colloids

1 Introduction

Several methods of characterization of magnetic colloidal dispersions —which consist of ultrafine magnetic particles dispersed in organic solvents and are known as magnetic fluids or ferrofluids— have been applied [1,2]. They exploit different physical properties of magnetic fluids like optical, rheological, magnetic or dielectric ones, often the magnetic field influence on them being investigated. Consequently, magnetic properties are fundamental for all types of investigations, but the magnetization curves can be extensively used for studying both particle interactions and aggregate formation, as done in this paper. For such a purpose, polydispersity, dipole-dipole interaction and chain-like cluster formation of magnetic nanoparticles, which may affect the magnetization curves resulting in deviation from the classical ideal (Langevin) theory, were taken into account.

Previous studies, which made use of magnetization measurements for sample characterization, were mainly focused on magneto-granulomteric analysis on ideal polydisperse ferrofluids [3] or interacting particle ferrofluids [4, 5] and on size distribution determination [6,7].

In this paper, in addition to the interaction of particles described by various models, we studied the possibility of chain-like aggregate formation, not done before even for the case of concentrated magnetic fluids [4]. The agreement between all used models and experimental data was carefully investigated before any quantative determinations, unlike in the previous studies mentioned.

Due to the complex problem of elaborating agglomeration models, many simplifying hypotheses are necessary and hence their limited applicability, which is not straightforward. One can take into account, for example, that the magnetic properties in the low-field region are mainly determined by the larger particles or aggregates (Fig. 1), for trying the agglomeration models.

Three series of dilutions of three types of ferrofluids containing magnetite particles, based on different organic solvents and stabilized with different surfactants, were prepared for this study.

2 Theoretical background

The various models for ferrofluid magnetization, used in Sections 3-5, are summarized in this section.

[a] e-mail: m.rasa@chem.uu.nl

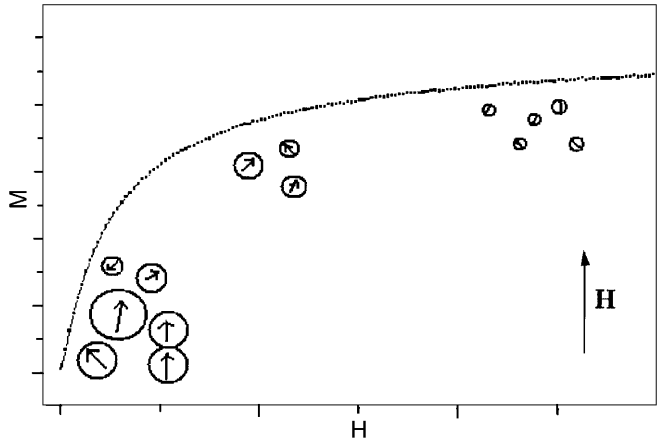

Fig. 1. Contribution to the magnetization process of particles with different sizes. In the low-field region mainly larger particles align their magnetic moment to the field direction and aggregate formation is most probable. At high fields, mainly the magnetic-moment orientation of small particles increases the magnetization.

The simplest model for the magnetization of a ferrofluid assumes Brownian monodisperse non-interacting spheres, having a permanent dipolar magnetic moment m which rotates together with the particles after applying an external magnetic field. This model is known as the ideal or Langevin model and the magnetization is given by $M = M_{\rm s}L(\xi)$ [1], where $L(\xi)$ is the so-called Langevin function defined as $L(\xi) = \coth\xi - 1/\xi$. ξ is the Langevin parameter, given by $\xi = \mu_0 mH/(k_{\rm B}T)$, where H is the applied field, μ_0 is the magnetic permeability of vacuum, $k_{\rm B}$ is Boltzmann's constant and T is the absolute temperature. The saturation magnetization $M_{\rm s}$ can be written as

$$M_{\rm s} = M_{\rm d}p_{\rm m}\Phi. \tag{1}$$

Here $M_{\rm d}$ is the spontaneous magnetization of particles, Φ is the physical volume fraction of dispersed solid and $p_{\rm m}$ is the ratio between the magnetic volume fraction $\Phi_{\rm m}$ and physical volume fraction Φ. The ideal (Langevin) initial susceptibility is given by

$$\chi_{\rm iL} = \frac{\mu_0\pi M_{\rm d}^2 D_{\rm m}^3 \Phi_{\rm m}}{18k_{\rm B}T}, \tag{2}$$

where $D_{\rm m}$ is the magnetic diameter of the particles.

A first correction can be done by including the polydispersity of particles, rather high, as resulted from a previous work [8]. It was also shown there that the lognormal size distribution,

$$f(x) = \frac{1}{xS\sqrt{2\pi}}\exp\left(-\frac{\ln^2\frac{x}{D_0}}{2S^2}\right), \tag{3}$$

is suitable for the type of magnetic fluids studied in this paper, so that it will be used further on. D_0 is defined by $\ln D_0 = \langle\ln x\rangle$, and S as the mean deviation of $\ln x$ from its mean value. x is the magnetic diameter. The two parameters of the distribution, D_0 and S, should be experimentally determined. The Langevin formula becomes

$$M = n\int_0^\infty m(x)L(\xi(x))f(x)\mathrm{d}x\,, \tag{4}$$

where n is the particle number density.

Dipole-dipole interaction influence on ferrofluid magnetism was studied in the framework of several models [9–12]. The thermodynamic perturbation theory (TPT) [9] applies for dilute and medium-concentrated ferrofluids, for which the dipole-dipole energy is smaller than the thermal energy:

$$M = n\int_0^\infty m(x)\left(\coth\xi - \frac{1}{\xi}\right)f(x)\mathrm{d}x \times\left[1 + \frac{n\mu_0}{3k_{\rm B}T}\int_0^\infty m^2(x)\left(\frac{1}{\xi^2} - \frac{1}{\sinh^2\xi}\right)f(x)\mathrm{d}x\right]. \tag{5}$$

The size distribution was included. The initial susceptibility, in the frame of this theory, is given by

$$\chi_{\rm i} = \chi_{\rm iL}\left(1 + \frac{1}{3}\chi_{\rm iL}\right), \tag{6}$$

where $\chi_{\rm iL}$ is the initial susceptibility in the absence of interactions. Such an expression can be used in the case of both monodisperse and polydisperse particles. If monodispersed particles are considered, then $\chi_{\rm iL}$ will be given by equation (2), otherwise it should be calculated using equation (4) [8].

Recently, a formula for the initial susceptibility for more concentrated ferrofluids was derived by the same author [10], using the same perturbation theory, but in the second order:

$$\chi_{\rm i} = \chi_{\rm iL}\left(1 + \frac{1}{3}\chi_{\rm iL} + \frac{1}{144}\chi_{\rm iL}^2\right). \tag{7}$$

The saturation magnetization, $M_{\rm s}$, can be determined using the asymptotic expression of magnetization of equation (5) for the high-field region:

$$M \cong M_{\rm s} - \frac{c}{H} + M_{\rm s}\frac{c}{3H^2} - \frac{c^2}{3H^3}\,, \tag{8}$$

where $c = nk_{\rm B}T/\mu_0$. If particles are monodisperse and the correction term in equation (5) is negligible, then equation (5) reduces to ideal magnetization, the initial susceptibility to $\chi_{\rm iL}$, and the high-field magnetization to $M \cong M_{\rm s} - c/H$.

The initial susceptibility is given by relatively simple formulas in the frames of other models too. Thus, Onsager's effective field theory (EFT), which considers that a particle is subjected to an effective field consisting of a "cavity field" proportional to the applied field and a "reaction field" proportional to the particle moment and dependent on its instantaneous orientation [11], gives

$$\chi_{\rm i} = \frac{3}{4}\left(\chi_{\rm iL} - 1 + \sqrt{1 + \frac{2}{3}\chi_{\rm iL} + \chi_{\rm iL}^2}\right). \tag{9}$$

The solution [13] of the generalized Onsager effective field theory [12] is known as the mean spherical model (MSM) and yields for the initial susceptibility [13]

$$\chi_{\mathrm{i}} = \frac{\chi_{\mathrm{iL}}}{q(-b)}\,, \tag{10}$$

where $q(b) = (1+2b)^2/(1-b)^4$. The parameter b can be found by solving the equation $\chi_{\mathrm{iL}} = q(2b) - q(-b)$, where $0 < b < 0.5$. The first three terms in equation (8) are also predicted by MSM.

Many times, the dipole-dipole interaction results in aggregate formation. Chain-like aggregate formation in the presence of the magnetic field as well as in zero field is theoretically modeled in [14]. This model will be referred to as the rod-shaped chain formation model (RCFM), since only rod-like chains were taken into account. The conditions $\epsilon \gg 1$ and $\epsilon \gg \xi$ were imposed. ϵ is the coupling parameter between two particles:

$$\epsilon = \frac{\mu_0 M_{\mathrm{d}}^2 V_{\mathrm{m}}^2}{2\pi D_{\mathrm{h}}^3 k_{\mathrm{B}} T}\,. \tag{11}$$

Here D_{h} is the hydrodynamic diameter of particles (obtained after adding the surfactant thickness to the physical diameter) and V_{m} is the magnetic volume of particles (determined by the magnetic diameter which is obtained after subtracting the thickness of the nonmagnetic layer from the physical diameter). The applicability of this model is also limited by neglecting the chain-chain interactions, so that it is not suitable for concentrated ferrofluids. Due to neglecting the chain shape fluctuations, the quantitative results are reliable if the condition $\langle k\rangle < \epsilon$ is fulfilled ($\langle k\rangle$ is the mean number of particles per chain). The initial susceptibility within the RCFM theory is given by

$$\chi_{\mathrm{i}} = \frac{\chi_{\mathrm{iL}}}{\Phi_{\mathrm{m}}} \exp(-\epsilon) \frac{x_0(1+x_0)}{(1-x_0)^3}\,, \tag{12}$$

where

$$x_0 = \frac{1 + 2\Phi_{\mathrm{m}} \exp(\epsilon) - \sqrt{1 + 4\Phi_{\mathrm{m}} \exp(\epsilon)}}{2\Phi_{\mathrm{m}} \exp(\epsilon)}\,. \tag{13}$$

The mean number of particles per cluster in the case of a very low field ($H \to 0$) can be calculated with

$$\langle k_0\rangle = \frac{\Phi_{\mathrm{m}} \exp(\epsilon)(1-x_0)}{x_0}\,. \tag{14}$$

The magnetization of a ferrofluid can be written as

$$M = m \sum_k kL(k\xi) g_k\,, \tag{15}$$

where g_k is the density of chains with k particles:

$$g_k = \frac{x^k}{V_{\mathrm{m}}} \frac{\sinh(\xi k)}{\xi k} \exp(-\epsilon) \tag{16}$$

in which

$$x = \frac{2y\cosh\xi + \sinh\xi - \sqrt{(2y\cosh\xi + \sinh\xi)^2 - 4y^2}}{2y} \tag{17}$$

with

$$y = \xi \Phi_{\mathrm{m}} \exp(\epsilon)\,. \tag{18}$$

In [15], a theory of particle chaining in zero field (CZF) was proposed. Chain flexibility is taken into account and the theory is applicable even for concentrated ferrofluids, but ϵ must be greater than one. Since the expression of initial susceptibility in [15] contains an error, we applied the following more general equation:

$$\chi_{\mathrm{i}} = \frac{1}{3k_{\mathrm{B}}T} \sum_k \langle m_k^2\rangle f_k\,, \tag{19}$$

where $\langle m_k^2\rangle$ is the mean squared magnetic moment of a k-particle chain. In the case of a rod-shaped chain, we have $\langle m_k^2\rangle = (mk)^2$. Otherwise, according to [15],

$$\langle m_k^2\rangle = 2\epsilon^2 m^2 \left(\frac{k}{\epsilon} - 1 + \exp\left(-\frac{k}{\epsilon}\right)\right)\,. \tag{20}$$

In equation (19), f_k is the density of chains with k particles:

$$f_k = \frac{\alpha^k}{V_{\mathrm{m}} \lambda k!} \tag{21}$$

in which α is the solution of equation $\alpha \exp\alpha = \lambda \Phi_{\mathrm{m}}$, and λ is given by

$$\lambda(\epsilon) = \frac{16}{9} \exp(\epsilon)[\epsilon \exp(-\epsilon)(Ei(\epsilon) - Ei(1) + 4e) - (1 + \epsilon^{-1} + 2\epsilon^{-2})]\,, \tag{22}$$

$Ei(\epsilon)$ being the second exponential integral.

3 Dilution series approach

The saturation magnetization, initial susceptibility, full reduced magnetization curves (M/M_{s}) and magneto-granulometric results (mean magnetic diameter $\langle D_{\mathrm{m}}\rangle$ and standard deviation σ) are all analyzed as a function of volume fraction, for each series of dilutions, as described in this section. The below proposed steps for qualitative and quantitative interpretation of these curves constitute the dilution series approach. The results and discussions for the particular case of our samples, all containing magnetite particles, are presented in Section 5.

We assume that the polydispersity is the same for each sample in a dilution series. This is achieved after a successive dilution process (starting from the most concentrated ferrofluid of one type) and can be also verified experimentally. If a comparison between the different ferrofluids is intended (as in this paper), then the ferrofluids (with different solvents and surfactants) should also have the same particle size distribution. This can be checked experimentally by performing electron microscopy.

The initial susceptibility can be influenced by many factors: particle diameter and size distribution, particle interactions, preformed aggregates (in the preparation process) and aggregate formation at zero field or induced by

the applied field. Therefore, $M_s = M_s(\Phi)$ curves are analyzed first, because their slope is determined by the single-particle distribution only (according to Eqs. (1) and (24)). $M_s = M_s(\Phi)$ are also useful for checking the accuracy of dilutions and of saturation magnetization determinations. They are used for determining the magnetic volume fraction and p_m. Later on, the nonmagnetic layer thickness can be determined, by using equation (24), after calculating the moments of the magnetic diameter. If the $M_s = M_s(\Phi)$ curves coincide for different series, then a comparison among the magnetic fluids can be done, since, in this case, the curves $\chi_i = \chi_i(\Phi)$ are influenced by the microstructural properties only.

By using the linear part of the initial susceptibility curves ($\chi_i = \chi_i(\Phi)$), as well as the value for p_m previously determined, the "initial" magnetic diameter, D_{mi}, (an effective magnetic diameter of larger particles which have the main contribution to the sample magnetization at low fields) can be obtained. Following a similar approach used in [16], the TPT, EFT, MSM, and in addition, RCFM, and CZF models (presented in Sect. 2), can be used for calculating the initial susceptibility and for interpreting the deviation from the linear behaviour of the curves $\chi_i = \chi_i(\Phi)$, at higher volume fractions. The agreement of these models with experimental data can be thus studied and then the influence of particle interactions and agglomerations might be quantified.

We anticipate that RCFM and CZF might not be applicable to our systems due to the small values of ϵ, which can be obtained if one takes into account the average diameter over all particles. They cannot also be adapted for polydisperse systems. However, in the low-field region mainly the larger particle subsystem contributes to the magnetization; this subsystem will be considered as a monodispersed one with the effective diameter D_{mi}, previously determined. At such a diameter, the effective coupling parameter, ϵ, is larger and could be determined experimentally (as a fit parameter). At room temperature, ϵ is mainly influenced by the proper particle grafting as well as by the particle polydispersity and surfactant compression. Thus, for a given distribution of particles, the value of ϵ is an indication of the stabilization quality. With the determined value of ϵ, the chain distribution function and the mean number of particles per aggregate can be calculated.

The reduced magnetization curves and their superposition, as well as $M = M(H)$ curves (having Φ as a parameter) are then qualitatively and quantitatively analyzed, respectively. Magneto-granulometry is performed using the magnetization curves of the most diluted samples, where interactions and agglomerations are negligible. Moments of the magnetic diameter of particles can be found at this stage. After applying the same magneto-granulometric technique for the entire range of volume fractions, the $\langle D_m \rangle = \langle D_m \rangle(\Phi)$ and $\sigma = \sigma(\Phi)$ dependences are analyzed. A dependence of these quantities on volume fraction would indicate changes in microstructural properties of samples with concentration, but at this stage the analysis is performed by using the entire magnetization curves (not only the low-field region as above).

Table 1. Magnetic-fluid samples. TR30 is the transformer oil, Pent the pentanol, POA the pure oleic acid, TOA the technical grade oleic acid and DBS the dodecyl-benzene-sulphonic acid.

Sample	Solvent	Surfactant	Volume fraction range (%)
1	TR30	POA	0.024–15.1
2	TR30	TOA	0.025–12.3
3	Pent	POA+DBS	0.020–17.6

4 Experimental

The magnetic fluids under investigation are presented in Table 1 and were prepared by following the procedure described in [17]. The first layer of surfactant (oleic acid) was chemisorbed on magnetite particles and then the free surfactant was eliminated. For pentanol-based samples a second surfactant is necessary and it was physically adsorbed on purified oleic acid. Successive dilutions were made with pure solvent. The volume fraction Φ of dispersed particles was determined from mass density measurements according to the equation

$$\Phi = \frac{\rho_{MF} - \rho_S}{\rho_P - \rho_S}, \tag{23}$$

where ρ_{MF} is the density of magnetic fluid, ρ_S is the density of carrier liquid and ρ_P is the density of solid particles. Magnetite particles were prepared by chemical coprecipitation [17] and were dispersed in different solvents according to Table 1. Electron micrographs showed the same particle size and distribution, close to the lognormal distribution, with a mean physical diameter $\langle D \rangle = 8.6$ nm, for all three types of samples. This fact is also investigated in the next section by using magnetization measurements only.

Measurements were done with a VSM (Vibrating Sample Magnetometer, LakeShore 7300) and an AGM (Alternating Gradient Magnetometer, MicroMag 2900) at room temperature. AGM is more sensitive, allowing the measurements of the lowest volume fraction samples.

In the case of VSM, a cylindrical sample holder was used and a correction for demagnetizing field was necessary. We used the demagnetizing factor for zero initial susceptibility, as discussed in a previous work [8].

In the case of very diluted samples measured with AGM, a correction for diamagnetism (mainly due to the sample holder) was necessary. For this purpose we fitted the measured curve with equation (5) to which the term $-\chi_{dia}H$ was added. Correction for demagnetizing field is not necessary in this case because of the very thin paralellipipedical shape of the sample holder (the narrow section is perpendicular to the magnetic field).

A very good superposition of the reduced curves of the same samples measured with the two magnetometers was obtained and exemplified in Figure 2. In this figure,

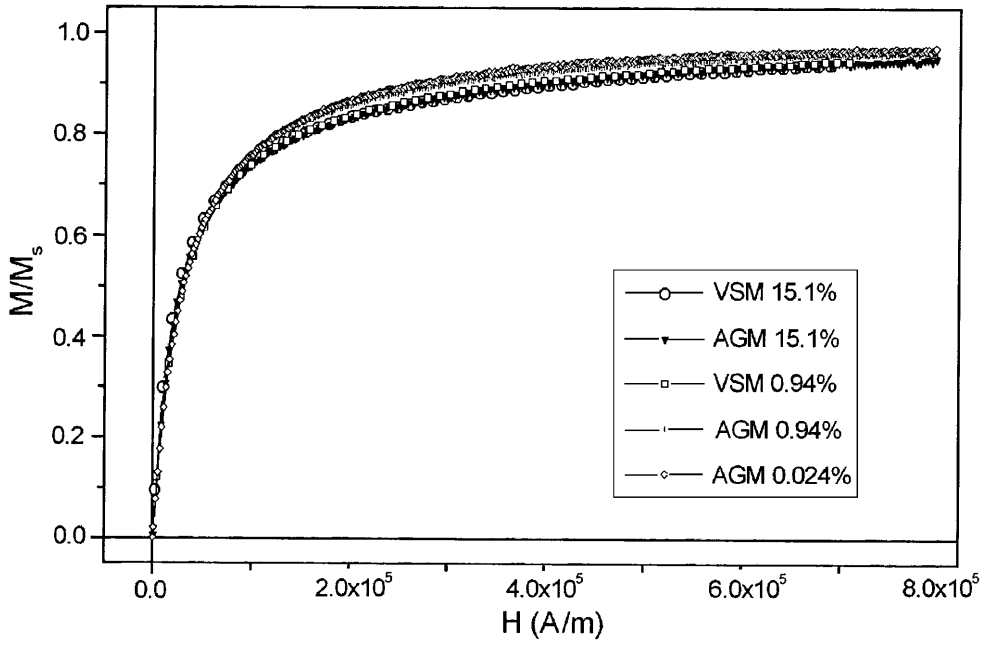

Fig. 2. Reduced magnetization curves of two different volume fractions of TR30+POA ferrofluid, measured with AGM and VSM techniques, indicating a very good agreement bewteen the two measurement techniques.

the sample with $\Phi = 0.024\%$ was measurable only with AGM. The deviation in the case of this sample is due the difference in microstructural properties of samples with different volume fractions, as discussed in the next section.

5 Results and discussions

Saturation magnetizations were determined from the quasi-saturation part of each $M = M(1/H)$ curve by fitting with a line. The results are presented in Figure 3. The linearity of $M_\mathrm{s} = M_\mathrm{s}(\Phi)$ is observed for all samples and the superposition of the curves is good, so that we expect the same mean volumes of particles dispersed in the three samples. This is because the slope of the $M_\mathrm{s} = M_\mathrm{s}(\Phi)$ curves depends only on p_m (given by Eq. (24)). Electron microscopy results are thus confirmed. The linearity of the curves also proves the accuracy of the dilution technique and of M_s determination. The analysis of fit residuals and the fit with the interacting model (Eq. (8)) showed that the quasisaturation part of the magnetization curves is indeed linear. The values obtained with equation (8) differ from those obtained with the line fit with 0.2% for the most concentrated samples, but the difference is much lower than the experimental reproducibility. For other volume fractions the values are practical identical. By fitting the $M_\mathrm{s} = M_\mathrm{s}(\Phi)$ curves with equation (1), p_m was determined (Tab. 2). Using the moments of the magnetic diameter of particles, determined later on in the paper, the thickness of the nonmagnetic layer δ was found using

$$p_\mathrm{m} = \frac{\langle D_\mathrm{m}^3 \rangle}{\langle (D_\mathrm{m} + \delta)^3 \rangle} \,. \qquad (24)$$

The results are also presented in Table 2.

Initial susceptibility curves, presented in Figure 4, show a linear behaviour at very low volume fractions only. The values of D_mi were determined after a line fit to the susceptibility in the very low fraction region, using equation (2) (Tab. 2). It is worth mentioning that the values for D_mi do not coincide for the three series of samples, in spite of the fact that the distribution of particles is the same. Since, at very low fractions, the samples exhibit a non-interacting behaviour, also confirmed in [16] for a similar sample based on cyclohexane, we conclude that, in this case, after applying a low field, the susceptibility is determined by the orientation of single particles and of small clusters formed in the absence of the field. More clusters are present in the case of TOA stabilized samples, due to the shorter length of acid tails, as well as due to the weak solvation of saturated acids, in comparison with POA. The weak solvation may reduce the steric repulsion leading to agglomerate formation. The presence of clusters in TOA samples in zero field, which results in a larger value for D_mi, is confirmed by the qualitative interpretations of rheological measurements in [5]. POA stabilized samples have a somewhat smaller value of D_mi than the one obtained for TOA samples, in agreement with the

Table 2. Results of various data processing.

Sample	p_m	δ (nm)	D_mi (nm)	ϵ
1	0.74	0.9	10.5	1.18
2	0.72	1.0	11.2	1.26
3	0.72	0.9	10.0	(< 1)

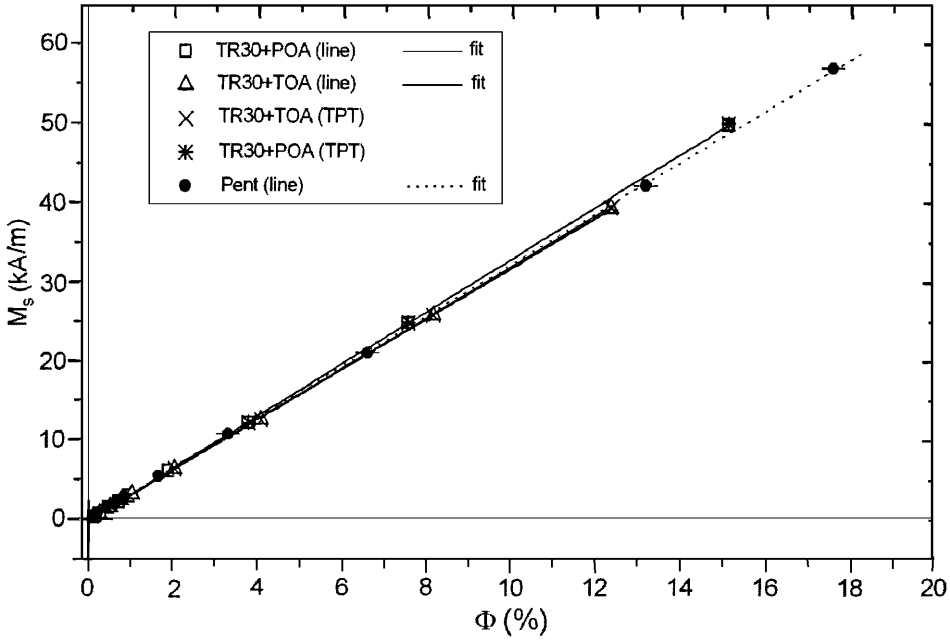

Fig. 3. Saturation magnetization *versus* physical volume fraction for the three series of dilutions. M_s is determined from a line fit to the quasi-saturation part of magnetization curves, and, for comparison, from a fit with TPT model (Eq. (8)). A good superposition is observed, evidencing the same polydispersity of particles.

above explanation. The lowest value of D_{mi} was obtained for pentanol-based samples and this is explained by the efficient reduction of interparticle interaction and thus of cluster formation due to the double layer of surfactant used. At higher volume fractions, the initial susceptibility varies non-linearly (Fig. 4). This can be due to both particle interactions and chain formation at higher fractions. They have the strongest influence in the case of TOA stabilized samples and the weakest one for Pent samples.

Using the values of D_{mi}, previously determined, equations (2,7,9,10) and (12) were represented on the same plot with the experimental data, in Figure 5 for POA stabilized samples based on TR30, and in Figure 6 for pentanol-based samples. In equation (11) and further on in the paper, the values of nonmagnetic layer of magnetite particles were taken from Table 2, and of the surfactant thickness from [18].

For the simple stabilized samples, all models underestimate the full curve $\chi_{\mathrm{i}} = \chi_{\mathrm{i}}(\Phi)$. TPT, MSM and RCFM give similar values for the initial susceptibility which are closest to the data points. EFT gives a stronger underestimation. The non-linearity is obvious above $\Phi_{\mathrm{m}} = 2\%$. For Pent-based samples, the calculated susceptibilities with TPT and MSM almost fit the measured susceptibilities and give similar results. Consequently, in the case of pentanol-based samples TPT and MSM describe well the experimental facts, and aggregation of particles seems to play a negligible role in the non-linearity of initial susceptibility of this type of ferrofluid. However, in the case of simple stabilized samples, in addition to interactions, small aggregates also influence the initial susceptibility. This can be also regarded as follows: equation (7) is not dependent on the stabilization method (it is a universal equation for ferrofluids). Consequently, the thickness of the surfactant does not play any role within the frame of this model, but it plays an important role in aggregate formation, so that the difference observed between TR30 and Pent samples is due to aggregate formation.

To have an estimation of the last type of contribution, we fitted the experimental data presented in Figures 5 and 6 with RCFM, having ϵ as a single fit parameter. The values obtained for simple stabilized samples are only slightly greater than one (Tab. 2) and are an indication of a very weak aggregation process. A determination of the mean number of particles per aggregate by using equation (14), in this case, is not possible due the limiting hypothesis of the model (discussed in Sect. 2). However, there are some facts which are worth mentioning. The fit with RCFM was very good and the value of ϵ determined from fit is very close to the real one, determined by using

$$\chi_{\mathrm{iL}} = 4\epsilon\Phi_{\mathrm{m}}\frac{D_{\mathrm{h}}^3}{D_{\mathrm{m}}^3}\,. \tag{25}$$

Equation (25) results after rewriting equation (2). After a fit to the low-fraction region of the susceptibility data with equation (25) we obtained $\epsilon = 1.17$ for POA stabilized samples. Using the determined ϵ with RCFM, the calculated magnetization with RCFM is close to the data, the deviation being up to 8% for ferrofluids with the volume fraction up to 3.7% in the low-field region (up to $6{\times}10^3$ A/m). Figure 5 also shows a qualitatively good compatibility between the initial susceptibility data and RCFM (as good as for MSM and TPT). RCFM model was also successful in explaining qualitatively the static magnetic dichroism of similar samples [19]. These show,

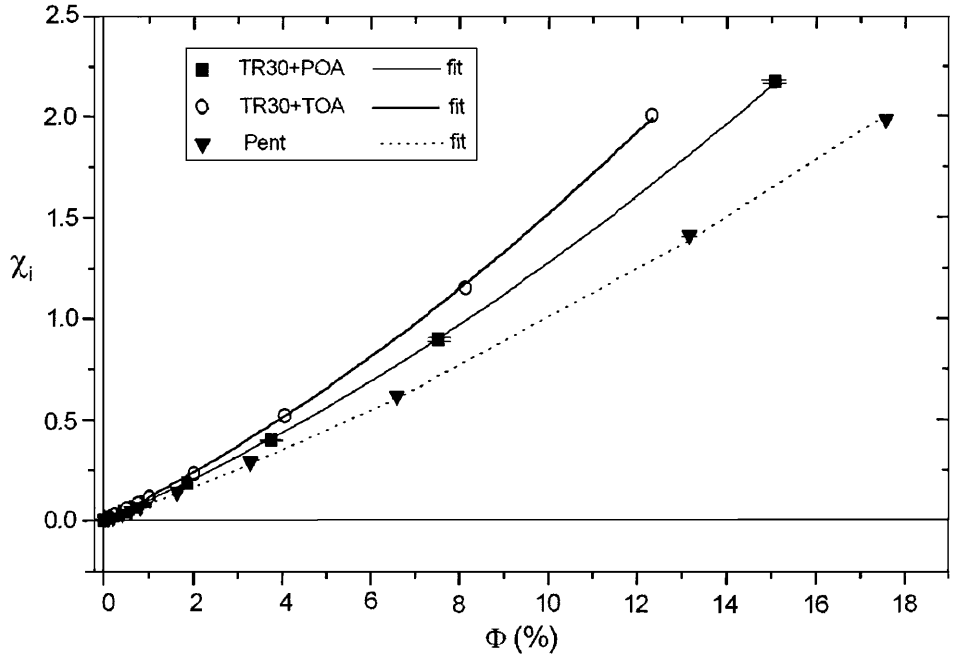

Fig. 4. Initial susceptibility *versus* physical volume fraction for the three series of dilutions. The non-linear behaviour can be a result of both particle interactions and aggregate formation in the samples. A preliminary fit with equation (7) is shown.

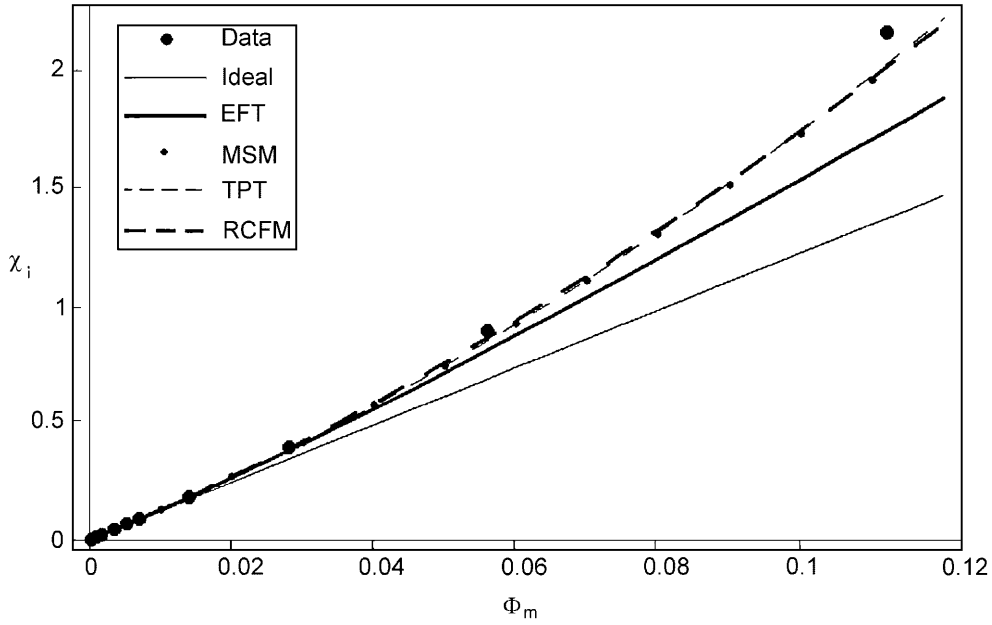

Fig. 5. Measured initial susceptibility for TR30+POA, and calculated initial susceptibilities with various models *versus* magnetic volume fraction. TPT, MSM and RCFM give values closest to the data.

surprisingly, that RCFM can be tried for an intuitive image of microstructure formation in these samples, and possible explanations are given in the next paragraph. Using RCFM, we found 1.1 particles per aggregate on the average, as an order of magnitude, for the POA sample with volume fraction of 3.7%. Figure 7 shows the chain distributions computed with RCFM and CFZ for the same TR30+POA sample in zero field. Because ϵ is small, the values obtained should be interpreted as a *possible scenario* of microstructures. However, we can conclude two things: a) in this limiting case, the two models give results close to each other for short chains, and b) with each new particle added to a chain, to form a $k+1$ particle chain, the density g_{k+1} decreases with one order of magnitude. For more concentrated samples, of course, we expect somewhat longer chains, but the chain-chain interaction has the effect of reducing the mean length of chains in comparison to those predicted by RCFM [20].

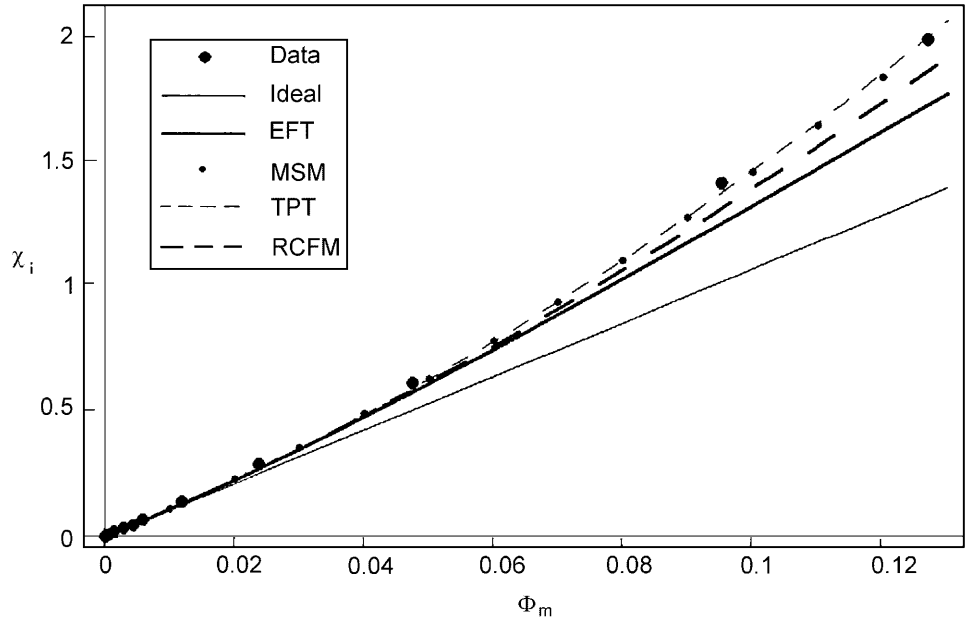

Fig. 6. Measured initial susceptibility for Pent samples, and calculated initial susceptibilities with various models *versus* magnetic volume fraction. For Pent-based samples the deviation from ideal behaviour is mainly due to particle interactions; TPT and MSM almost fit the data.

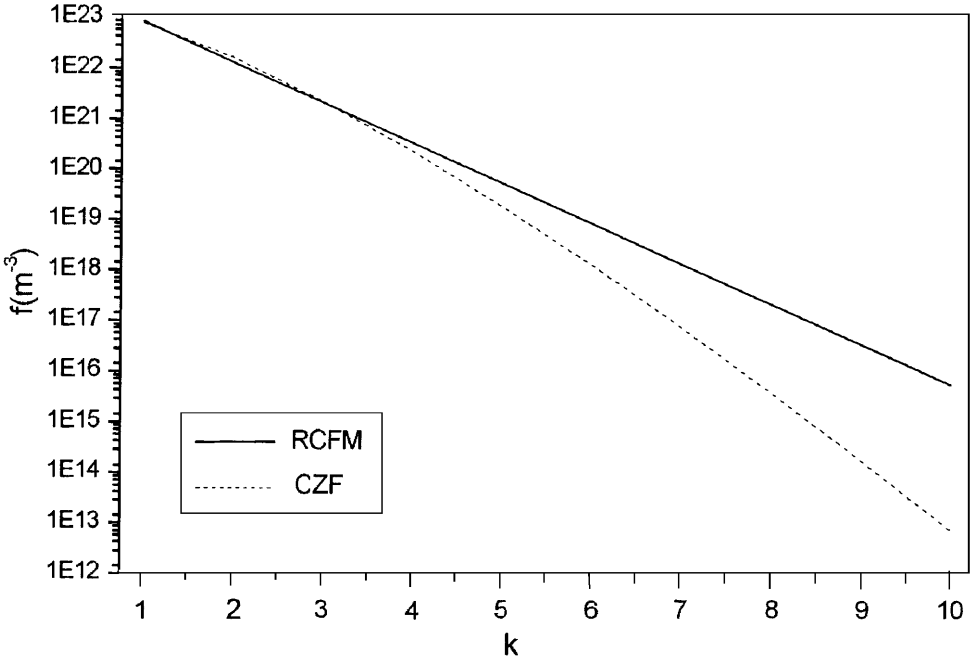

Fig. 7. Density of chain distribution *versus* number of particles per chain in zero field calculated with RCFM and CZF for TR30+POA sample with $\Phi = 3.7\%$ for the limiting case of small coupling constant. The two models give similar chain distribution functions only in the short-chain region.

In the case of using flexible-chain hypothesis, equations (19) together with (20) did not fit the data well; the way in which flexibility is taken into account in CZF is also problematic since polymers usually form very long chains in comparison with what is expected in the majority of ferrofluids. This might suggest that, referring to the models used, a better qualitative description of our samples is given if short and rigid chains are considered. Probably the chains contain mainly the largest particles of the size distribution, as well as particles not properly grafted with surfactant (and hence a stronger coupling between them than the one indicated by the effective value of ϵ).

However, as discussed above, a part of the deviation from ideal behaviour is due to single-particle interactions, so that the chains have a *smaller effect* on magnetization curves than the one described by RCFM only. It is not

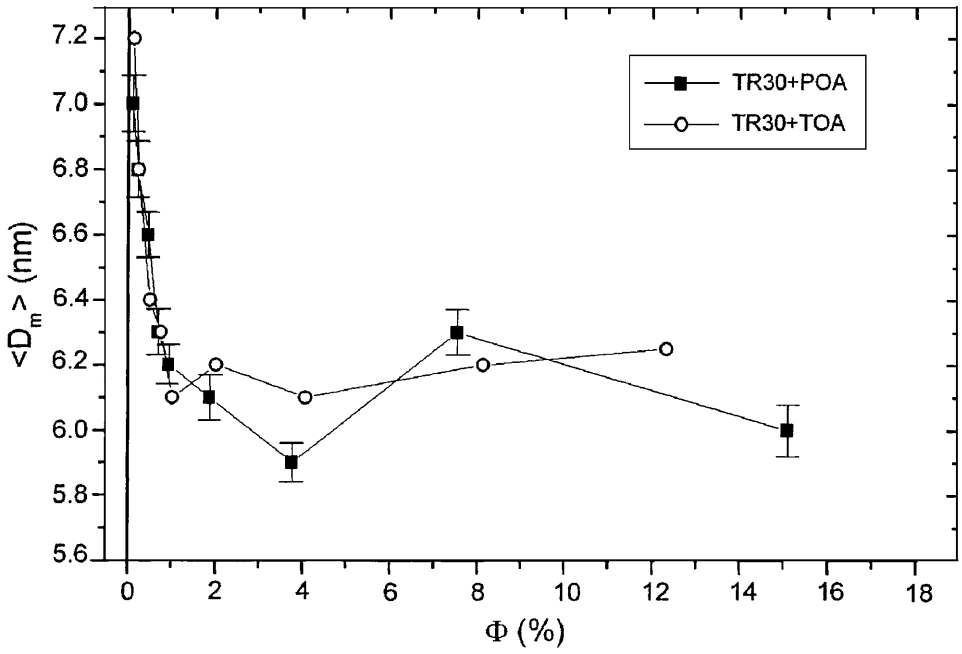

Fig. 8. Unexpected dependence of mean magnetic diameter *versus* physical volume fraction.

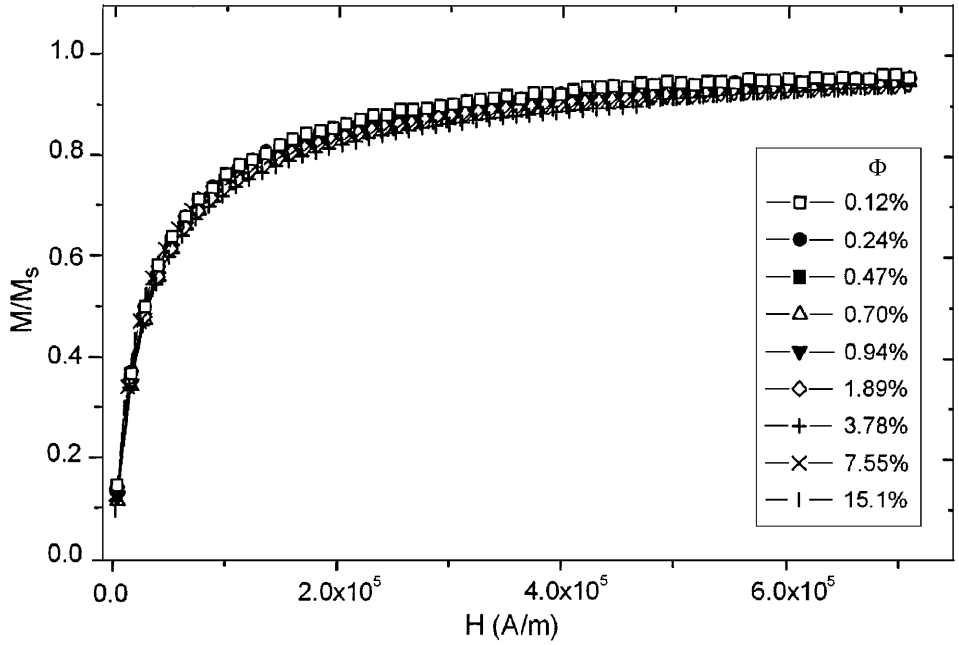

Fig. 9. Reduced magnetization curves of TR30+POA series having the physical volume fraction as a parameter. The curves intersect each other, but their superposition is quite good for such a large volume fraction range.

possible to separate the contribution of particle interactions and chain formation to the magnetic properties of these samples.

In comparison with the susceptibility data published in [21], the initial susceptibilities of our ferrofluids are much smaller at similar volume fractions. It is not clear in [21] what the mean diameter of magnetite particles corresponding to data presented in Figure 1 is and how it was determined, but some general assertions in the paper show that it is comparable to ours. In this case it means that those samples are aggregated. It remains a problem to understand how MSM and TPT could describe those samples as well.

For the double-surfacted pentanol-based samples, the RCFM would fit this curve for a value of ϵ below one. This is a confirmation of the above conclusions about pentanol, concerning the negligible presence of aggregates. We recall finally that all the discussions up to now are valid for

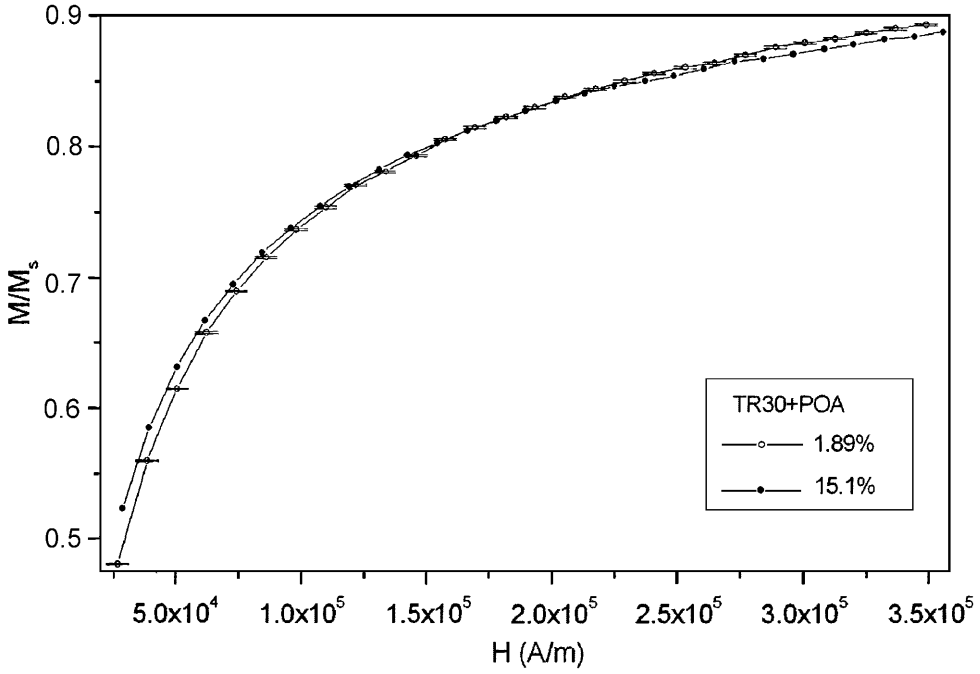

Fig. 10. An example of intersection point between two reduced magnetization curves.

the low-field region and for the particles which determine the ferrofluid behaviour in this region. For higher fields, interparticle interactions and aggregations play a less and less important role because of the stronger interactions of single particles with the external field.

The magneto-granulometric analysis was performed first on the most dilute samples, to determine the the mean magnetic diameter of single particles, by using the entire $M = M(H)$ curves and the formulas derived in a previous work [5] (in order to avoid the fit with multiple parameters):

$$S = \frac{1}{3}\sqrt{\ln\frac{3\alpha H_0}{M_\mathrm{s}}}\,, \tag{26}$$

$$D_0^3 = \frac{6k_\mathrm{B}T}{\mu_0\pi H_0 M_\mathrm{d}}\sqrt{\frac{M_\mathrm{s}}{3\alpha H_0}}\,, \tag{27}$$

$$n = \frac{\mu_0 H_0 M_\mathrm{s}}{k_\mathrm{B}T}\,, \tag{28}$$

where $\alpha = (\sqrt{9+12\chi_\mathrm{i}} - 3)/2$. For non-interacting particles $\alpha = \chi_\mathrm{i}$. H_0 is the intersection with the abscissa of the quasi-linear part of the magnetization curve, in the representation $M = M(1/H)$. With the aid of the lognormal distribution parameters, S and D_0, given by equations (26) and (27), the mean magnetic diameter $\langle D_\mathrm{m}\rangle$ and the standard deviation σ can be computed as in [5]. The polydispersity was around 36%. The result (Fig. 8) is in very good agreement with the mean physical diameter (8.6 nm) determined from TEM. Further on, the magneto-granulometry analysis was extended to all fractions. Figure 8 shows the dependence of mean magnetic diameters for the TR30-based samples *versus* volume fraction. One can observe the decreasing of $\langle D_\mathrm{m}\rangle$ with Φ, which was not expected. The effect is doubtless in the case of TR30 samples up to fractions of 2-4%, but is was very small and below determination errors in the case of pentanol-based samples. The standard deviation of diameters for the samples analyzed fluctuates between certain limits but is not particularly dependent on Φ.

After analyzing the reduced magnetization curves (all determined with VSM, in the same conditions —Fig. 9), we concluded that the results shown in Figure 8 are consequences of determination artifacts: the reduced curves show systematically an intersection point, which is not explained by the interacting models and thus not included in equations (26-27). In fact, none of the models used in this paper applied within their range of validity, predict such an intersection point. Both AGM and VSM measurements exhibit such an intersection. An example is given in Figure 10. The determination of saturation magnetization is correct according to Figure 3 and to the discussions in the first paragraph in Section 5. However, it is interesting to notice that the quasi-saturation part of the reduced magnetization curves varies with $1/H$ but does not obey the ideal (Langevin) model: from Figure 9, one can observe that the slope of the quasi-saturation part of the reduced magnetization curves increases with the volume fraction. Consequently, this part of the curve is properly described by the following equation of magnetization:

$$M = M_\mathrm{s} - \frac{c(\Phi)}{H}\,, \tag{29}$$

where c, within the frame of the Langevin model, was defined in Section 2.

Qualitatively, a possible explanation of this fine effect of intersection is a result of volume-fraction–dependent small-aggregate formation with polydisperse particles in

the presence of the external field, at low fields only. Agglomeration process rapidly saturates because, at higher fields, the particle interaction with the external field is stronger than the interactions between particles. At high fields, thus, even chain disruption may occur and more single particles will orient to saturate the magnetization curve (explaining also Eq. (29)).

The probability of chaining increases with the volume fraction and, consequently, smaller particles may become part of clusters [22] (in a probable configuration in which larger particles are in the middle of the chains). Consequently, as the volume fraction increases, only smaller and smaller independent particles of the size distribution will contribute to the magnetization process at a certain (higher) field, lowering the reduced curve at higher fields, of a certain sample, below the one corresponding to a lower volume fraction. In fact, the above considerations suggest that the effect could be explained if polydispersity were taken into account in the agglomeration models. We recall the fact that polydispersity together with interacting models do not explain this intersection. Unfortunately, the magnetic field corresponding to the intersection point is too high for trying RCFM on the subsystem of large particles. Speculations on van der Waals interactions only seem not to be suitable for explaining this effect: the polydispersity of particles in the ferrofluids has a negligible influence on van der Waals energy of two spheres in comparison with the influence on the corresponding dipole-dipole energy (the particles are considered coated with a 2 nm surfactant layer). The possible preformed aggregates, coupled by van der Waals attraction, are present in all samples due to the successive dilution and their presence is not a result of a fraction-dependent formation process. The moment distribution in such a van der Waals cluster is usually arbitrary so that the net moment is zero. At small fields, it is not obvious that the presence of such clusters increases the susceptibility. Such interactions are possible between particles not properly grafted, but the main role in the microstructural effects of our ferrofluids is played by the longer-range dipole-dipole interactions, as resulted from the initial susceptibility analysis.

6 Conclusions

Using $M_\mathrm{s} = M_\mathrm{s}(\Phi)$ together with $\chi_\mathrm{i} = \chi_\mathrm{i}(\Phi)$ curves, we conclude that, at very low volume fractions, there is an ideal magnetic behaviour, but the initial susceptibility in this region is also determined by small clusters formed in the absence of the magnetic field. The TOA stabilized samples contain slightly larger aggregates than the POA stabilized samples in zero field, while in the case of pentanol-based samples (with a double layer of surfactant) the presence of aggregates is negligible. This is due to the type and quality of surfactants used. In the higher-fraction region, both particle interactions and small chain formation explain the $\chi_\mathrm{i} = \chi_\mathrm{i}(\Phi)$ curves for simple stabilized samples. In the case of double surfacted samples, only particle interactions were found significant. Thermodynamic perturbation theory (TPT) and mean spherical model (MSM) are closest to the data but slightly underestimate the susceptibility in the case of simple stabilized samples. Effective field theory (EFT) gives a stronger underestimation in all cases.

Despite the very small values of the coupling parameters, the rod-shaped chain formation model (RCFM) gave a reasonable scenario for the microstrucure formation for TR30 samples, short and rigid chains being possible. However, it is not suitable for quantitative analysis of our samples. By using the susceptibility data only it is not possible to separate the contribution of particle interactions and aggregates.

The presence of aggregates in the case of double-surfacted samples was inferred to be very small, with a negligible effect on their static magnetic properties. Consequently, from the microstructural point of view, the analyzed samples are high-quality ferrofluids.

The magneto-granulometry, performed on the most diluted samples, and $M_\mathrm{s} = M_\mathrm{s}(\Phi)$ curves allowed the calculation of the nonmagnetic-layer thickness. After performing statistics on particles for all dilutions, the $\langle D_\mathrm{m}\rangle = \langle D_\mathrm{m}\rangle(\Phi)$ curves showed an unexpected dependence on volume fraction for TR30 samples. In this cases an intersection point between the reduced magnetization curves was observed. It is not explained by any of the interacting models or aggregation models referred in this paper, so that the dependence of the mean magnetic diameter on volume fraction is a determination artifact. We also noticed that the quasi-saturation part of the reduced magnetization curves varies with $1/H$ but does not obey the ideal (Langevin) model. A possible explanation is due to the volume-fraction–dependent chain formation with polydisperse particles in low fields, which rapidly saturates as the field increases. The need of a chain formation model with polydisperse particles valid for higher magnetic fields and weakly interacting particles is thus obvious.

As a final note, we mention that the large variety of magnetite ferrofluids with respect to particle size distribution and structures as well as stabilization makes it at present still difficult to draw conclusions about the general applicability of the models. This warrants ongoing efforts to synthesize more well-defined magnetic colloids (iron or cobalt particles, for example).

We thank to Dr. G. van Ewijk and Dr. G. J. Vroege (Van 't Hoff Lab.) and Prof. A. Yu. Zubarev (Ural State University) for helpful discussions. We would like to thank to the Romanian Academy of Science for the partial financial support for Dr. Doina Bica and Dr. L. Vékás through the research grants supervised by Prof. I. Anton in 2000 and 2001.

References

1. B. Berkovski, V. Bashtovoi (Editors), *Magnetic Fluids and Applications Handbook*, (Begell House, 1996).
2. M. Raşa, D. Bica, L. Vékás, Ann. Univ. Petrosani, Phys. Ser. **2**, 3 (2000).

3. R.W. Chantrell, J. Popplewell, S.W. Charles, IEEE Trans. Magn. **14**, 975 (1978).
4. A.F. Pshenichnikov, V.V. Mekhonoshin, A.V. Lebedev, J. Magn. & Magn. Mater. **161**, 94 (1996).
5. L. Vékás, M. Raşa, D. Bica, J. Colloid. Interface Sci. **231**, 247 (2000).
6. R.M. Asimow, Trans. Met. Soc. AIME **233**, 401 (1965)
7. D.V. Berkov, A. Daum, P. Goernert, N. Buske, C. Gansau, J. Mueller, M. Giersig, W. Neumann, D. Su, IEEE Trans. Magn. **35**, 4064 (1999).
8. M. Raşa, Eur. Phys. J. E **2**, 265 (2000).
9. A.O. Ivanov, Magn. Gidr. **4**, 39 (1992).
10. A.O. Ivanov, O.B. Kuznetsova, Colloid J. **63**, 60 (2001).
11. L. Onsager, J. Am. Chem. Soc. **58**, 1486 (1936).
12. J.G. Kirkwood, J. Chem. Phys. **7**, 911 (1939).
13. M.S. Wertheim, J. Chem. Phys. **55**, 4291 (1971).
14. A.Yu. Zubarev, L.Yu. Iskakova, Zh. Eksp. Teor. Fiz. **107**, 1543 (1995).
15. M. Shliomis, in *Abstracts of the Eighth International Conference on Magnetic Fluids*, edited by I. Anton, L. Vékás, V. Sofonea (Mirton Press, Timişoara, 1998) p. 10.
16. G. van Ewijk, Ph.D. Thesis, Utrecht University, 2000.
17. D. Bica, Rom. Rep. Phys. **47**, 265 (1995).
18. L. Vékás, D. Bica, D. Gheorghe, I. Potencz, M. Raşa, J. Magn. & Magn. Mater. **201**, 159 (1999).
19. V. Socoliuc, J. Magn. & Magn. Mater. **207**, 146 (1999).
20. L.Yu. Iskakova, A.Yu. Zubarev, submitted to Phys. Rev. E.
21. A.F. Pshenichnikov, J. Magn. & Magn. Mater. **145**, 319 (1995).
22. S. Kantorovich, A.O. Ivanov, in *Abstracts of the Ninth International Conference on Magnetic Fluids, Bremen, 2001.*